Inorganic Chemistry
Article

Inorg. Chem. 2010, 49, 7129–7134 7129
DOI: 10.1021/ic100948m

Effects of Counter Anions on Intense Photoluminescence of 1-D Chain Gold(I) Complexes

Masashi Saitoh,[†] Alan L. Balch,[‡] Junpei Yuasa,[†] and Tsuyoshi Kawai*[,†]

[†]*Graduate School of Materials and Science, Nara Institute of Science and Technology, NAIST, 8916-5 Takayama, Ikoma, Nara 630-0192, Japan, and* [‡]*Department of Chemistry, University of California, Davis, California 95616*

Received May 12, 2010

A series of cationic carbene complexes of Au(I) with different types of counteranions, $[Au\{C(OMe)NHMe\}_2]^+(X^-)$ (X^- = $CF_3SO_3^-$, PF_6^-, $CF_3CO_2^-$, ClO_4^-, and I^-), was synthesized, and their intense photoluminescence was studied. These complexes crystallize in the same space group, and the X-ray crystallographic data of these samples revealed the short Au(I)−Au(I) aurophilic distances (3.263−3.335 Å), where planar carbene Au(I) complexes are organized into linear stacks. The aurophilic Au(I)−Au(I) interactions found in the crystalline state give rise to phosphorescence with relatively high emission quantum efficiencies, whereas $[Au\{C(OMe)NHMe\}_2]^+(X^-)$ complexes show no appreciable emission in solutions. The Au(I)−Au(I) distances in the crystal of $[Au\{C(OMe)NHMe\}_2]^+(X^-)$ vary depending on the type of counteranions because the carbene ligands of Au(I) cations are linked through hydrogen bonds with adjacent counteranions. The effects of counteranions on the Au(I)−Au(I) aurophilic interactions allow one to modulate the intense photoluminescence color from blue to yellow by adjusting the counteranions of $[Au\{C(OMe)NHMe\}_2]^+(X^-)$ complexes.

Introduction

Luminescent metal complexes with relatively high emission quantum yields have attracted considerable attention as light emissive materials for the use in various molecular-based devices.[1−3] Especially, light-emitting metal complexes with near-unity quantum yields serve as wavelength conversion materials capable of emitting light of a color different from that of the excited light.[4,5] In this case, systematic preparation of metal complexes with different emission color is generally required to cover wide wavelength ranges. In the case of highly emissive iridium(III) and ruthenium(III) complexes [e.g., $Ru(bpy)_3^{2+}$ and $Ir(ppy)_3^{3+}$ derivatives], their excitation and emission maxima can be tuned by adjusting the energy of the excited states, when a judicious choice of ligands surrounding the metal center makes it possible to modulate the energy of the highest occupied molecular orbital (HOMO) levels.[6,7] On the other hand, the photophysical properties of Au(I) complexes with a d^{10} electronic configuration possess intense and long-lived photoluminescence. In these cases, the photophysical features result from the overlap of filled d orbitals and empty p orbitals on Au(I) cation, when the Au(I) cation forms an aurophilic bond with the adjacent two Au(I) cations within the complexes[8−12] or in the crystalline states.[13−15] As a consequence of the Au(I)−Au(I) aurophilic interaction, Au(I) cations are often found to have solid-state structural arrangements possessing one-dimensional (1-D) Au(I) chains. For example, Au(I) complexes

*To whom correspondence should be addressed. Phone: +81-743-72-6170. Fax: +81-743-72-6179. E-mail: tkawai@ms.naist.jp.

(1) (a) Amendola, V.; Fabbrizzi, L.; Foti, F.; Licchelli, M.; Mangano, C.; Pallavicini, P.; Poggi, A.; Sacchi, D.; Taglietti, A. *Coord. Chem. Rev.* **2005**, *250*, 273–299. (b) Evans, R. C.; Douglas, P.; Winscom, C. J. *Coord. Chem. Rev.* **2006**, *250*, 2093–2126.

(2) (a) Baldo, M. A.; O'Brien, D. F.; You, Y.; Shoustikov, A.; Sibley, S.; Thompson, M. E.; Forrest, S. R. *Nature* **1998**, *395*, 151–154. (b) Baldo, M. A.; Lamansky, S.; Burrows, P. E.; Thompson, M. E.; Forrest, S. R. *Appl. Phys. Lett.* **1999**, *75*, 4–6. (c) Adachi, C.; Baldo, M. A.; Forrest, S. R.; Thompson, M. E. *Appl. Phys. Lett.* **2000**, *77*, 904–906. (d) Nazeeruddin, Md. K.; Humphry-Baker, R.; Berner, D.; Rivier, S.; Zuppiroli, L.; Graetzel, M. *J. Am. Chem. Soc.* **2003**, *125*, 8790–8797.

(3) Grätzel, M. *Nature* **2001**, *414*, 338–344.

(4) House, J. E. *Descriptive Inorganic Chemistry*; Academic Press: New York, 2008.

(5) Moore, E. G.; Samuel, A. P. S.; Raymond, K. N. *Acc. Chem. Res.* **2009**, *42*, 542–552.

(6) (a) Juris, A.; Balzani, V.; Barigelletti, F.; Campagna, S.; Belser, P.; von Zelewsky, A. *Coord. Chem. Rev.* **1988**, *84*, 85–277. (b) Balzani, V.; Juris, A.; Venturi, M.; Campagna, S.; Serroni, S. *Chem. Rev.* **1996**, *96*, 759–834.

(7) Williams, J. A. G. *Chem. Soc. Rev.* **2009**, *38*, 1783–1801.

(8) (a) Hao, L. J.; Lachicotte, R. J.; Gysling, H. J.; Eisenberg, R. *Inorg. Chem.* **1999**, *38*, 4616–4617. (b) Lee, Y. A.; McGarrah, J. E.; Lachicotte, R. J.; Eisenberg, R. *J. Am. Chem. Soc.* **2002**, *124*, 10662–10663.

(9) Takemura, Y.; Takenaka, H.; Nakajima, T.; Tanase, T. *Angew. Chem., Int. Ed.* **2009**, *48*, 2157–2161.

(10) Barnard, P. J.; Wedlock, L. E.; Baker, M. V.; Berners-Price, S. J.; Joyce, D. A.; Skelton, B. W.; Steer, J. H. *Angew. Chem., Int. Ed.* **2006**, *45*, 5966–5970.

(11) Lu, X.; Yavuz, M. S.; Tuan, H. Y.; Korgel, B. A.; Xia, Y. *J. Am. Chem. Soc.* **2008**, *130*, 8900–8901.

(12) Jia, J. H.; Wang, Q. M. *J. Am. Chem. Soc.* **2009**, *131*, 16634–16635.

Published on Web 06/28/2010

with planar carbene ligands, $[Au\{C(NHMe)_2\}_2]^+(X^-)$ had been found to form 1-D Au(I) chain structures in the crystalline state.[16] In these systems, their excitation and emission maxima are suggested to be determined by the Au(I)−Au(I) distance.[17−21]

This unique optical property of the Au(I) complexes allows one to modulate excitation and emission maxima by changing their environment around the Au(I)−Au(I) bond by, for example, doping/dedoping in organogels[22] and solvent effects in the Au(I) binuclear complex.[23] If one can maintain the excellent emission quantum yield of the Au(I) complexes irrespective of changes in the aurophilic interaction[24,25] and the associated wavelength shifts, it would expand the scope of the availability of the Au(I) complexes for intensely luminescent materials. In such a case, however, the aurophilic interaction would have to be delicately tuned by adjusting the environment around the Au(I)−Au(I) bond.

In the present study, we demonstrate that the emission color of $[Au\{C(OMe)NHMe\}_2]^+(X^-)$ varies from blue to yellow depending on the type of counteranions ($X^- = CF_3SO_3^-$, PF_6^-, $CF_3CO_2^-$, ClO_4^-, and I^-) [Chart 1], whereas all of the $[Au\{C(OMe)NHMe\}_2]^+(X^-)$ complexes have specifically high phosphorescence quantum yields, Φ_{PL} (73−99%) in the crystalline state. Emission quantum yields of a series of the 1-D chain Au(I) complexes with different counteranions were determined for the first time. The systematic X-ray studies of the crystal structures of $[Au\{C(OMe)NHMe\}_2]^+(X^-)$ with the same space group revealed that the Au(I)−Au(I) distances in the crystalline state are well regulated by the steric hindrance of the counteranion because the carbene ligands form hydrogen-bonds between the adjacent counteranions.

Chart 1

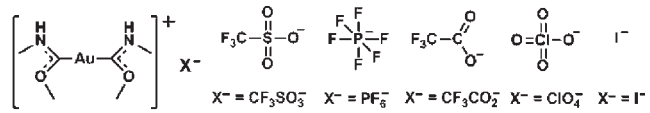

$[Au\{C(OMe)(NHMe)\}_2]^+(X^-)$

Experimental Section

Apparatus. All crystallographic data were obtained with a Rigaku RAXIS RAPID imaging plate detector with graphite-monochromated Mo−K_α radiation (λ = 0.71073 Å). The data were corrected at a temperature of 153 ± 1 K to a maximum 2θ value of 48.8°. Corrections for decay and Lorentz-polarization effects were made with empirical absorption correction and solved by direct methods and expanded using Fourier techniques. The non-hydrogen atoms were refined anisotropically. Hydrogen atoms were refined using the riding model. The final cycle of full-matrix least-squares refinement was based on observed reflections and variable parameters. ^{1}H NMR was obtained with a JEOL AL-300 spectrometer. Matrix-assisted laser desorption ionization time-of-flight mass spectrometry (MALDI-TOF mass) was performed using a DE-STR Voyager MALDI-TOF mass spectrometer. Elemental analyses were performed with a Perkin-Elmer 2400II. The stationary photoluminescence spectra were measured on a JASCO F-6500 spectrofluorometer. The photoluminescence microscopy images were obtained using Olympus fluorescence microscopy with an Olympus imaging camera (DP-20). Photoluminescence lifetime measurements were performed using a picoseconds luminescence measurement system (Hamamatsu C4780) with a streak scope (Hamamatsu C4334). The excitation source was generated by a Nd:YVO_4 laser (COHERENT, VERDI) pumped Ti:sapphire laser system (COHERENT, MIRA-900) equipped with a cavity dumper (COHERENT, PulseSwitch). This system delivers 100 fs pulse trains at 740 nm and runs at a repetition rate of 10 kHz for the time-resolved photoluminescence measurements. After the frequency was doubled with a LiB_3O_5 crystal, the incident pulses were focused on the sample. The power of the laser irradiation was less than 100 nW, whose value was optimized for avoiding thermal degradation of samples.

Materials. All reagents and starting materials are commercially available from Tokyo Chemical Industry Co., Ltd. and were used without further purification. Literature procedures were used for preparation of chloro(tetrahydrothiophene)gold(I) [Au(tht)Cl][26] and methyl isocyanide (MeNC).[27]

General Synthetic Procedure of $[Au\{C(OMe)NHMe\}_2]^+(X^-)$ Complexes ($X^- = CF_3SO_3^-$, PF_6^-, $CF_3CO_2^-$, ClO_4^-, and I^-). The preparation of Au(I) complexes, $[Au\{C(OMe)NHMe\}_2]^+(X^-)$ [$X^- = CF_3SO_3^-$, PF_6^-, $CF_3CO_2^-$, ClO_4^-, and I^-], involved the reaction of Au(tht)Cl with MeNC followed by adding sodium salts, Na^+X^- ($X^- = CF_3SO_3^-$, PF_6^-, $CF_3CO_2^-$, ClO_4^-, and I^-) in methanol. The resulting precipitates were collected by evaporation and dried under reduced pressure to give analytically pure $[Au\{C(OMe)NHMe\}]_2]^+(X^-)$ complexes as an air-stable solid, which are soluble in common organic solvents. These complexes were characterized by ^{1}H NMR, MALDI-TOF mass, and elemental analysis.[28] Recrystallization of $[Au\{C(OMe)NHMe\}_2]^+(X^-)$ [$X^- = CF_3SO_3^-$, PF_6^-, $CF_3CO_2^-$, ClO_4^-, and I^-] from dichloromethane afforded single crystals suitable for the photoluminescence measurement and the single-crystal X-ray structural analysis.

(13) (a) Yam, V. W. W.; Lo, K. K. W. In *Multimetallic and Macromolecular Inorganic Photochemistry*; Ramamurthy, V., Schanze, K. S., Eds.; Molecular and Supramolecular Photochemistry; Marcel Dekker: New York, 1999; Vol. *4*, pp 31−112. (b) Yam, V. W. W.; Lo, K. K. W. *Chem. Soc. Rev.* **1999**, *28*, 323–334. (c) Yam, V. W. W.; Cheng, E. C. C. *Chem. Soc. Rev.* **2008**, *37*, 1806–1813.

(14) Forward, J. M.; Fackler, J. P., Jr.; Assefa, Z. Photophysical and Photochemical Properties of Au(I) Complexes. In *Optoelectronic Properties of Inorganic Compounds*; Roundhill, D. M., Fackler, J. P., Jr., Eds.; Plenum Press: New York, 1999; pp 195−229.

(15) Balch, A. L. *Struct. Bonding* (*Berlin*) **2007**, *123*, 1–40.

(16) (a) White-Morris, R. L.; Olmstead, M. M.; Jiang, F.; Balch, A. L. *Inorg. Chem.* **2002**, *41*, 2313–2315. (b) Rios, D.; Pham, D. M.; Fettinger, J. C.; Olmstead, M. M.; Balch, A. L. *Inorg. Chem.* **2008**, *47*, 3442–3451.

(17) Rawashdeh-Omary, M. A.; Omary, M. A.; Patterson, H. H.; Fackler, J. P., Jr. *J. Am. Chem. Soc.* **2001**, *123*, 11237–11247.

(18) Tong, G. S. M.; Kui, S. C. F.; Chao, H. Y.; Zhu, N.; Che, C. M. *Chem.—Eur. J.* **2009**, *15*, 10777–10789.

(19) (a) Assefa, Z.; McBurnett, B. G.; Staples, R. J.; Fackler, J. P., Jr.; Assmann, B.; Angermaier, K.; Schmidbaur, H. *Inorg. Chem.* **1995**, *34*, 75–83. (b) Assefa, Z.; McBurnett, B. G.; Staples, R. J.; Fackler, J. P., Jr. *Inorg. Chem.* **1995**, *34*, 4965–4972. (c) Schneider, J.; Lee, Y. A.; Perez, J.; Brennessel, W. W.; Flaschenriem, C.; Eisenberg, R. *Inorg. Chem.* **2008**, *47*, 957–968. (d) Wakeshima, M.; Kato, M.; Tsuge, K.; Sawamura, M. *J. Am. Chem. Soc.* **2008**, *130*, 10044–10045.

(20) (a) Coker, N. L.; Bauer, J. A. K.; Elder, R. C. *J. Am. Chem. Soc.* **2004**, *126*, 12–13. (b) Arvapally, R. K.; Sinha, P.; Hettiarachchi, S. R.; Coker, N. L.; Bedel, C. E.; Patterson, H. H.; Elder, R. C.; Wilson, A. K.; Omary, M. A. *J. Phys. Chem. C* **2007**, *111*, 10689–10699.

(21) (a) White-Morris, R. L.; Olmstead, M. M.; Balch, A. L.; Elbjeirami, O.; Omary, M. A. *Inorg. Chem.* **2003**, *42*, 6741–6748. (b) Elbjeirami, O.; Omary, M. A.; Stender, M.; Balch, A. L. *Dalton Trans.* **2004**, 3173–3175.

(22) Kishimura, A.; Yamashita, T.; Aida, T. *J. Am. Chem. Soc.* **2005**, *127*, 179–183.

(23) (a) White-Morris, R. L.; Olmstead, M. M.; Jiang, F.; Tinti, D. S.; Balch, A. L. *J. Am. Chem. Soc.* **2002**, *124*, 2327–2336. (b) White-Morris, R. L.; Olmstead, M. M.; Balch, A. L. *J. Am. Chem. Soc.* **2003**, *125*, 1033–1040.

(24) (a) Schmidbaur, H. *Gold Bull.* **1990**, *23*, 11–21. (b) Schmidbaur, H.; Schier, A. *Chem. Soc. Rev.* **2008**, *37*, 1931–1951.

(25) Pyykkö, P. *Angew. Chem., Int. Ed.* **2004**, *43*, 4412–4456.

(26) Ahrland, S.; Dreish, K.; Norén, B.; Oskarsson, Å. *Mater. Chem. Phys.* **1993**, *35*, 281–289.

(27) Schuster, R. E.; Scott, J. F.; Casanova, J., Jr. *Org. Syntheses* **1966**, *46*, 75–76.

(28) Deprotonation of [C(OMe)NHMe] could take place under basic conditions. However, the deprotonated form $[C(OMe)NMe]^-$ was not obtained under the experimental conditions employed in this work.

Preparation of $[Au\{C(OMe)NHMe\}_2]^+(CF_3SO_3^-)$. To a solution of chloro(tetrahydrothiophene)gold(I) (0.17 g, 0.53 mmol) in 30 mL of methanol, methyl isocyanide (65 μL, 1.2 mmol) was added, and the reaction mixture was stirred for 15 min at room temperature. When the mixture turned clear completely, sodium trifluorosulfonate (0.81 g, 4.7 mmol) was added. After stirring for overnight, the solution was filtered and then the solvent was removed in a vacuum. The slightly yellow residue was obtained after removing the insoluble element in dichloromethane (0.25 g, 96% yield for two steps). This residue was taken up in dichloromethane and crystallized. ^{1}H NMR (300 MHz, $CDCl_3$): 9.72 (brs, 2H), 4.27 (s, 6H), 2.90 (d, J = 5.0 Hz, 6H). MALDI-TOF mass calcd. for $C_7H_{14}N_2O_5SF_3Au$: m/z 492.2. Found: m/z 343.3 $[M - CF_3SO_3]^+$. Anal. Calcd. for $C_7H_{14}N_2O_5SF_3Au$: C, 17.08; H, 2.87; N, 5.69. Found: C, 17.06; H, 2.61; N, 5.67.

Preparation of $[Au\{C(OMe)NHMe\}_2]^+(PF_6^-)$. To a solution of chloro(tetrahydrothiophene)gold(I), (0.15 g, 0.47 mmol) in 30 mL of methanol, methyl isocyanide (65 μL, 1.2 mmol) was added, and the reaction mixture was stirred for 15 min at room temperature. When the mixture turned clear completely, sodium hexafluorophosphate (0.39 g, 2.3 mmol) was added. After stirring for overnight, the solution was filtered, and then the solvent was removed in a vacuum. The slightly yellow residue was obtained after removing the insoluble element in dichloromethane (0.19 g, 82% yield for two steps). This residue was taken up in dichloromethane and crystallized. ^{1}H NMR (300 MHz, $CDCl_3$): 8.25 (brs, 2H), 4.29 (s, 6H), 2.94 (d, J = 5.0 Hz, 6H). MALDI-TOF mass calcd. for $C_6H_{14}AuF_6N_2O_2P$: m/z 488.1. Found: m/z 343.3 $[M - PF_6]^+$. Anal. Calcd. for $C_6H_{14}AuF_6N_2O_2P$: C, 14.76; H, 2.89; N, 5.74. Found: C, 14.88; H, 2.69; N, 5.89.

Preparation of $[Au\{C(OMe)NHMe\}_2]^+(CF_3CO_2^-)$. To a solution of chloro(tetrahydrothiophene)gold(I), (0.15 g, 0.47 mmol) in 30 mL of methanol, methyl isocyanide (65 μL, 1.2 mmol) was added, and the reaction mixture was stirred for 15 min at room temperature. When the mixture turned clear completely, sodium trifluoroacetate (0.32 g, 2.3 mmol) was added. After stirring for overnight, the solution was filtered, and then the solvent was removed in a vacuum. The slightly yellow residue was obtained after removing the insoluble element in dichloromethane (0.19 g, 90% yield for two steps). This residue was taken up in dichloromethane and crystallized. ^{1}H NMR (300 MHz, $CDCl_3$): 10.94 (brs, 2H), 4.23 (s, 6H), 2.90 (d, J = 5.0 Hz, 6H). MALDI-TOF mass calcd. for $C_8H_{14}N_2O_4F_3Au$: m/z 456.2. Found: m/z 343.3 $[M - CF_3CO_2]^+$. Anal. Calcd. for $C_8H_{14}N_2O_4F_3Au$: C, 21.06; H, 3.09; N, 6.14. Found: C, 20.98; H, 2.83; N, 6.11.

Preparation of $[Au\{C(OMe)NHMe\}_2]^+(ClO_4^-)$. To a solution of chloro(tetrahydrothiophene)gold(I), (0.15 g, 0.47 mmol) in 30 mL of methanol, methyl isocyanide (65 μL, 1.2 mmol) was added, and the reaction mixture was stirred for 15 min at room temperature. When the mixture turned clear completely, sodium perchlorate (0.29 g, 2.4 mmol) was added. ***Caution!*** *Perchlorate salts of metal complexes with organic ligands are potentially explosive in certain conditions and should be handled with appropriate care at all times*. After stirring for overnight, the solution was filtered and then the solvent was removed in a vacuum. The slightly yellow residue was obtained after removing the insoluble element in dichloromethane (0.19 g, 91% yield for two steps). This residue was taken up in dichloromethane and crystallized. ^{1}H NMR (300 MHz, $CDCl_3$): 4.28 (s, 6H), 2.92 (s, 6H). MALDI-TOF mass calcd. for $C_6H_{14}AuClN_2O_6$: m/z 442.6. Found: m/z 343.2 $[M - ClO_4]^+$. Anal. Calcd. for $C_6H_{14}AuClN_2O_6$: C, 16.28; H, 3.19; N, 6.33. Found: C, 16.44; H, 2.93; N, 6.43.

Preparation of $[Au\{C(OMe)NHMe\}_2]^+(I^-)$. To a solution of chloro(tetrahydrothiophene)gold(I) (0.15 g, 0.47 mmol) in 30 mL of methanol, methyl isocyanide (65 μL, 1.2 mmol) was added, and the reaction mixture was stirred for 15 min at room temperature. When the mixture turned clear completely, sodium iodide (0.47 g, 3.1 mmol) was added. After stirring for overnight, the solution was filtered, and then the solvent was removed in a vacuum. The yellow residue was obtained after removing the insoluble element in dichloromethane (0.18 g, 82% yield for two steps). This residue was taken up in dichloromethane and crystallized. ^{1}H NMR (300 MHz, $CDCl_3$): 9.90 (brs, 2H), 4.31 (s, 6H), 2.89 (d, J = 4.6 Hz, 6H). MALDI-TOF mass calcd. for $C_6H_{14}N_2O_2IAu$: m/z 470.0. Found: m/z 343.3 $[M - I]^+$. Anal. Calcd. for $C_6H_{14}N_2O_2IAu$: C, 15.33; H, 3.00; N, 5.96. Found: C, 15.24; H, 2.65; N, 6.35.

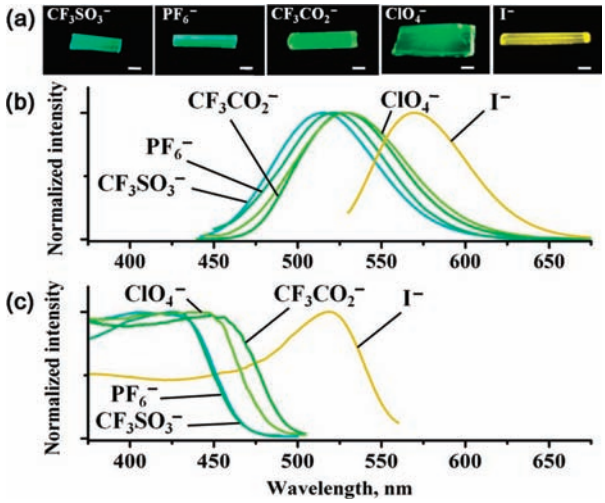

Figure 1. (a) Photographs of $[Au\{C(OMe)NHMe\}_2]^+(X^-)$ in the crystalline state under UV irradiation (365 nm) at room temperature (scale bar: 200 μm). Normalized (b) emission and (c) excitation spectra of $[Au\{C(OMe)NHMe\}_2]^+(X^-)$ in the crystalline state at room temperature.

Table 1. Photophysical Data of $[Au\{C(OMe)NHMe\}_2]^+(X^-)$ in the Crystalline State

X^-	$\lambda_{p\text{-}em}$ (nm)[a]	$\lambda_{p\text{-}ex}$ (nm)[b]	Φ_{PL} (%)[c]	τ (μs)[d]	k_r (s^{-1})[e]	k_{nr} (s^{-1})[f]
$CF_3SO_3^-$	514	406	98	2.4	4.1×10^5	8.3×10^3
PF_6^-	521	426	99	2.6	3.8×10^5	3.8×10^3
$CF_3CO_2^-$	527	448	92	2.3	4.0×10^5	3.5×10^4
ClO_4^-	530	442	96	2.0	4.8×10^5	2.0×10^4
I^-	570	517	73	1.6	4.6×10^5	1.7×10^5

[a] Excitation wavelength: 420 nm for $CF_3SO_3^-$, 425 nm for PF_6^-, 430 nm for $CF_3CO_2^-$, 442 nm for ClO_4^-, and 517 nm for I^-. [b] Monitor wavelength: 514 nm for $CF_3SO_3^-$, 521 nm for PF_6^-, 527 nm for $CF_3CO_2^-$, 530 nm for ClO_4^-, and 570 nm for I^-. [c] Emission quantum yields were determined with a calibrated integrating sphere system.[29,32] [d] Emission lifetimes of $[Au\{C(OMe)NHMe\}_2]^+(X^-)$ were measured under excitation at 370 nm. [e] Radiative rate constants were estimated with $k_r = \Phi_{PL}/\tau$. [f] Non-radiative rate constants were estimated with $k_{nr} = (1 - \Phi_{PL})/\tau$.

Emission Quantum Yield Determination. Emission quantum yields of $[Au\{C(OMe)NHMe\}_2]^+(X^-)$ crystals were determined by a JASCO F-6500 spectrofluorometer equipped with an integrating sphere,[29] JASCO ILF-533 (vide supra). The wavelength dependences of the detector response and the beam intensity of Xe light source for each spectrum were calibrated using a standard light source (Matsusada PK-80). The validity of the measuring emission quantum efficiencies was confirmed by reference standard for emission quantum yield, anthracene,[30] quinine sulfate,[31] and rhodamine B.[30]

Results and Discussions

Photoluminescence Measurements in the Crystalline State. Suitable crystals (a polygonal columnar shape with

(29) De Mello, C.; Wittmann, H. F.; Friend, R. H. *Adv. Mater.* **1997**, *9*, 230–232.
(30) Crosby, G. A.; Demas, J. N. *J. Phys. Chem.* **1971**, *75*, 991–1024.
(31) Melhuish, W. H. *J. Phys. Chem.* **1961**, *65*, 229–235.

Table 2. Crystallographic Data for $[Au\{C(OMe)NHMe\}_2]^+(X^-)$ Complexes

	$CF_3SO_3^-$	PF_6^-	$CF_3CO_2^-$	ClO_4^-	I^-
formula	$C_7H_{14}AuF_3N_2O_5S$	$C_6H_{14}AuF_6N_2O_2P$	$C_8H_{14}AuF_3N_2O_4$	$C_6H_{14}AuClN_2O_6$	$C_6H_{14}AuIN_2O_2$
formula weight	492.22	488.12	456.17	442.6	470.06
T, K	153.1	153.1	153.1	153.1	153.1
crystal system	orthorhombic	orthorhombic	orthorhombic	orthorhombic	orthorhombic
space group	P*nma*	P*nma*	P*nma*	P*nma*	P*nma*
a, Å	6.63559(15)	19.4920(11)	6.5698(3)	18.7988(6)	17.9751(7)
b, Å	13.7327(3)	6.6616(3)	13.5474(5)	6.59111(18)	6.5219(3)
c, Å	15.5183(4)	10.3329(5)	14.9227(7)	9.7619(4)	9.6332(5)
α, deg	90	90	90	90	90
β, deg	90	90	90	90	90
γ, deg	90	90	90	90	90
V, Å^3	1414.10(6)	1341.69(12)	1328.18(10)	1209.54(7)	1129.32(9)
Z	4	4	4	4	4
d, g·cm^{-3}	2.312	2.416	2.281	2.430	2.764
R1[a]	0.0218	0.0422	0.0357	0.0354	0.0278
wR2[b]	0.057	0.1064	0.0942	0.0923	0.0690

[a] $R1 = \sum||F_o| - |F_c||/\sum|F_o|$. [b] $wR2 = [\sum w(F_o^2 - F_c^2)^2/\sum w(F_o^2)^2]^{1/2}$.

the length to about 1.0 mm) of $[Au\{C(OMe)NHMe\}_2]^+(X^-)$ were grown by slow evaporation of CH_2Cl_2 solutions of $[Au\{C(OMe)NHMe\}_2]^+(X^-)$ complexes. Microscopic photographs of these crystals are shown in Figure 1a, in which all Au(I) crystals showed intense photoluminescence typical of multinuclear Au(I) ions linked with aurophilic interactions.[24,25] The emission color of these crystals was varied from blue to yellow depending on their counteranions: slightly bluish green emission for $CF_3SO_3^-$, green emission for PF_6^-, $CF_3CO_2^-$ and ClO_4^-, as well as yellow emission for I^- (Figure 1a). Accordingly, these crystals showed broad emission bands in a wide wavelength range (514−570 nm) [the emission maxima ($\lambda_{p\text{-}em}$): 514 nm for $CF_3SO_3^-$, 521 nm for PF_6^-, 527 nm for $CF_3CO_2^-$, 530 nm for ClO_4^- and, 570 nm for I^- (Figure 1b)]. Similarly, the excitation maxima of $[Au\{C(OMe)NHMe\}_2]^+(X^-)$ in the crystalline state were different depending on their counteranion parts [the excitation maxima ($\lambda_{p\text{-}ex}$): 406 nm for $CF_3SO_3^-$, 426 nm for PF_6^-, 448 nm for $CF_3CO_2^-$, 442 nm for ClO_4^-, and 517 nm for I^- (Figure 1c)]. In contrast, all $[Au\{C(OMe)NHMe\}_2]^+(X^-)$ complexes exhibit extremely high emission quantum yields (Φ_{PL}), 98% for $CF_3SO_3^-$, 99% for PF_6^-, 92% for $CF_3CO_2^-$, 96% for ClO_4^-, and 73% for I^-, which the extremely high quantum yields seem to be independent of the difference in their counteranion parts.[32]

We have also determined emission lifetimes of crystals of $[Au\{C(OMe)NHMe\}_2]^+(X^-)$. Time-resolved emission spectroscopy under pulsed excitation light showed single-exponential decays, providing the excited state lifetimes of 2.4 μs for $CF_3SO_3^-$, 2.6 μs for PF_6^-, 2.3 μs for $CF_3CO_2^-$, 2.0 μs for ClO_4^-, and 1.6 μs for I^- (see Supporting Information, Figure S3). The relatively long lifetimes in the microsecond range indicate phosphorescence from $[Au\{C(OMe)NHMe\}_2]^+(X^-)$ crystals followed by rapid intersystem crossing.[16] The radiative (k_r) and non-radiative (k_{nr}) rate constants were estimated from the emission lifetimes and the emission quantum yields.[33] The k_r of PF_6^- (3.8×10^5 s^{-1}) were similar to k_r of other counteranions in magnitude (4.1×10^5−4.8×10^5 s^{-1}). On the other hand, all samples show the relatively small k_{nr}, among them the $[Au\{C(OMe)NHMe\}_2]^+(PF_6^-)$ crystal showed the smallest k_{nr} value (3.8×10^3 s^{-1}), leading to the extremely high emission quantum yield (99%).[32]

Photophysical data of $[Au\{C(OMe)NHMe\}_2]^+(X^-)$ examined here are summarized in Table 1. As noted above, crystals of $[Au\{C(OMe)NHMe\}_2]^+(X^-)$ show a variety of emission color from blue to yellow depending on the type of counteranions (Figure 1), whereas the difference in counteranion parts of the $[Au\{C(OMe)NHMe\}_2]^+(X^-)$ complexes has no appreciable inference on their relatively high emission quantum yields (Table 1). The significant difference in the emission color of $[Au\{C(OMe)NHMe\}_2]^+(X^-)$ in the crystalline state depending on the counterion may be ascribed to the interaction of the $[Au\{C(OMe)NHMe\}_2]^+$ cation with the anion in the crystal lattice. Thus, we had examined the detailed X-ray crystal analysis of the $[Au\{C(OMe)NHMe\}_2]^+(X^-)$ complexes (vide infra).

Single-Crystal X-ray Structural Analyses. Crystallographic data for the $[Au\{C(OMe)NHMe\}_2]^+(X^-)$ complexes are shown in Table 2.[34] All crystal structures showed the same space group. The molecular structures and the molecular packing diagrams of $[Au\{C(OMe)NHMe\}_2]^+(X^-)$ with a series of counteranions are shown in Figure 2 and 3, respectively. The Au(I) metal center of $[Au\{C(OMe)NHMe\}_2]^+(X^-)$ are coordinated by two carbene ligands in a nearly linear fashion, where two carbene ligands have almost planar structures (Figure 2). The X-ray crystallographic data revealed that the N−H groups of the carbene ligands form hydrogen bonds in planar chelate rings to the oxygen atoms of $CF_3SO_3^-$ (Figure 2a), those to the fluorine atoms of PF_6^- (Figure 2b),[35] those to the oxygen atoms of $CF_3CO_2^-$ (Figure 2c), and those to I^- (Figure 2e). In the case of

(32) Although emission quantum yields of $[Au\{C(OMe)NHMe\}_2]^+(X^-)$ ($X^- = CF_3SO_3^-$, PF_6^-, $CF_3CO_2^-$, and ClO_4^-) crystals could contain unavoidable experimental (measuring) error of 1−2%, their emission quantum efficiencies of some crystals are close to unity.

(33) The quantum efficiency of intersystem crossing from singlet state to triplet state seems to be almost unity judging from the phosphorescence quantum efficiency of almost unity.

(34) The Au(I)−Au(I) distance of $[Au\{C(OMe)NHMe\}_2]^+(CF_3CO_2^-)$ in the crystalline state at 89 K were previously reported; See: Jiang, F.; Olmstead, M. M.; Balch, A. L. *J. Chem. Soc., Dalton Trans.* **2000**, 4098–4103; In this work, we have determined the Au(I)−Au(I) distances of all $[Au\{C(OMe)NHMe\}_2]^+(X^-)$ at 153 K.

(35) The PF_6 anion shows some disorder, whereas the structure of the cation $[Au\{C(OMe)NHMe\}_2]^+$ is clear. Disorder of PF_6 indicates weak hydrogen bond interactions with N−H of carbene ligands.

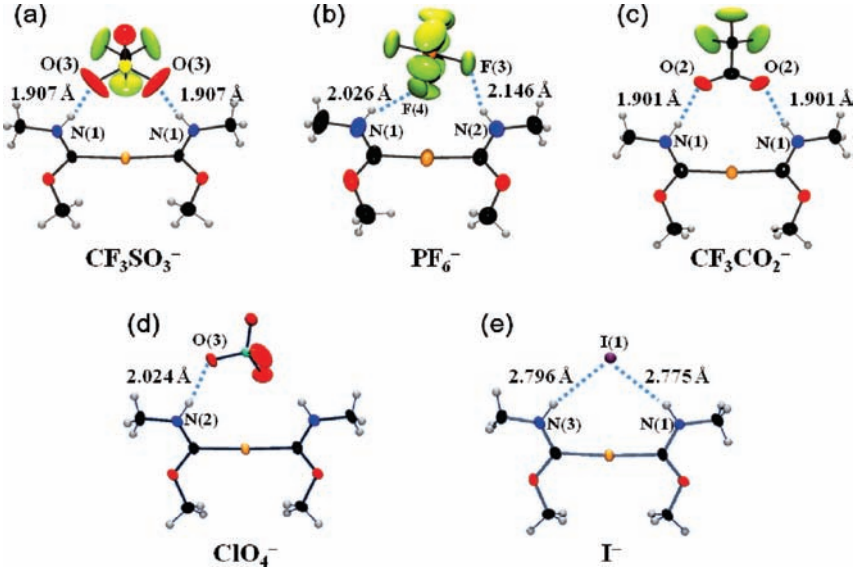

Figure 2. ORTEP drawing of (a) $[Au\{C(OMe)NHMe\}_2]^+(CF_3SO_3^-)$, (b) $[Au\{C(OMe)NHMe\}_2]^+(PF_6^-)$, (c) $[Au\{C(OMe)NHMe\}_2]^+(CF_3CO_2^-)$, (d) $[Au\{C(OMe)NHMe\}_2]^+(ClO_4^-)$, and (e) $[Au\{C(OMe)NHMe\}_2]^+(I^-)$. Blue dotted lines denote the hydrogen bonding interactions between the N−H groups of the carbene ligands and the counteranions.

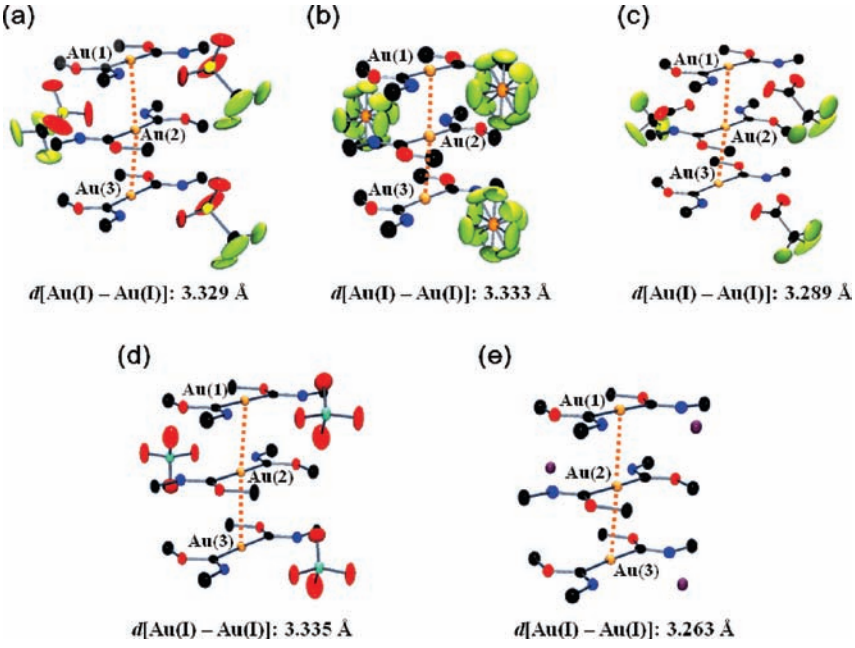

Figure 3. Molecular packing diagrams of the crystal structures of (a) $[Au\{C(OMe)NHMe\}_2]^+(CF_3SO_3^-)$, (b) $[Au\{C(OMe)NHMe\}_2]^+(PF_6^-)$, (c) $[Au\{C(OMe)NHMe\}_2]^+(CF_3CO_2^-)$, (d) $[Au\{C(OMe)NHMe\}_2]^+(ClO_4^-)$, and (e) $[Au\{C(OMe)NHMe\}_2]^+(I^-)$. Orange dotted lines denote aurophilic interactions. Hydrogen atoms are omitted for clarity.

$[Au\{C(OMe)NHMe\}_2]^+(ClO_4^-)$, the N−H group of the carbene ligand forms a monodentate hydrogen bond with the oxygen atom of ClO_4^- (Figure 2d). On the other hand, the individual cationic $[Au\{C(OMe)NHMe\}_2]^+$ units are organized into linear stacks (Figure 3),[36] where the Au(I) ion forms the aurophilic interactions between adjacent Au(I) centers (dashed lines in Figure 3). In the case of $[Au\{C(OMe)NHMe\}_2]^+(I^-)$, the $[Au\{C(OMe)NHMe\}_2]^+$ unit forms the almost linear 1-D chain structure [the Au(1)−Au(2)−Au(3) angle: 176.37° (Figure 4a)]. The linear 1-D chain structure was changed to the zigzag chain structure, when the counteranion of I^- was replaced by the more bulky ClO_4^- anion [the Au(1)−Au(2)−Au(3) angle: 162.39° (Figure 4b)], which lengthen the Au(I)−Au(I) distance (0.072 Å). The zigzag chain structure of $[Au\{C(OMe)NHMe\}_2]^+(ClO_4^-)$ should be ascribed to steric repulsion between the OMe group of carbene ligands and

(36) The shortest face-to-face distances for stacking between two adjacent carbene ligands were ranged from 3.265 Å to 3.344 Å [3.319 Å for $CF_3CO_2^-$, 3.331 Å for PF_6^-, 3.285 Å for $CF_3CO_2^-$, 3.344 Å for ClO_4^-, and 3.265 Å for I^-]. The C−Au−C axes within a stack are always parallel (dihedral angle between adjacent carbene ligands is 4.6° for $CF_3SO_3^-$, 4.2° for PF_6^-, 4.6° for $CF_3CO_2^-$, 2.2° for ClO_4^-, and 3.8° for I^-, respectively). The π-stacking interactions between the carbene ligands may provide additional stabilization for the 1-D chain structure, where adjacent carbene ligands interdigitate with one another.

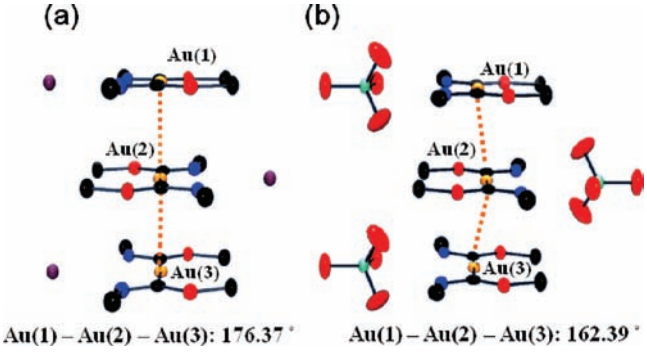

Figure 4. Molecular packing diagrams of linear chain structure of (a) $[Au\{C(OMe)NHMe\}_2]^+(I^-)$ and the zigzag 1-D chain structure of (b) $[Au\{C(OMe)NHMe\}_2]^+(ClO_4^-)$ in the crystalline state. Orange dotted lines denote aurophilic interactions. Hydrogen atoms are omitted for clarity.

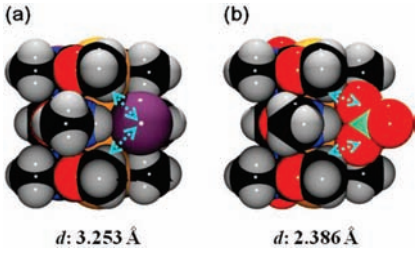

Figure 5. Space-filling views of (a) $[Au\{C(OMe)NHMe\}_2]^+(I^-)$ and (b) $[Au\{C(OMe)NHMe\}_2]^+(ClO_4^-)$ in the crystalline state.

the oxygen atoms of ClO_4^- (d = 2.386 Å), although there is no steric repulsion between the OMe group of carbene ligands and the iodine atom (d = 3.253 Å) [Figure 5]. Similarly, steric repulsion on the $CF_3SO_3^-$, PF_6^-, and $CF_3CO_2^-$ results in the zigzag chain structures [the Au(1)–Au(2)–Au(3) angle: 170.70° ($CF_3SO_3^-$), 175.70° (PF_6^-), and 174.46° ($CF_3CO_2^-$); see Supporting Information, Figures S4 and S5]. Thus, the steric hindrance of the counteranion affects the Au(I)–Au(I) distances in part when the individual cationic $[Au\{C(OMe)NHMe\}_2]^+$ units are tightly linked with their counteranion parts.[37]

The excitation and emission of the photoluminescence crystals of $[Au\{C(OMe)NHMe\}_2]^+(X^-)$ result from the aurophilic interactions between the Au(I) centers. In that case, the overlapping between the occupied $5d_{z^2}$ orbitals of two adjacent Au(I) metal centers produces filled valence bands composed of bonding, $d_{z^2}\sigma$, and antibonding, $d_{z^2}\sigma^*$, molecular orbitals, respectively.[38] Thus, the steric hindrance of the counteranion is expected to affect the overlapping between the $5d_{z^2}$ orbitals, resulting in excitation and emission variations from the $[Au\{C(OMe)NHMe\}_2]^+(X^-)$ complexes in the crystalline state.

(37) Emission and excitation wavelength maxima were suggested to be red-shifted with respect to a shorter Au(I)–Au(I) distance.[19a,b] In our case also, $[Au\{C(OMe)NHMe\}_2]^+(I^-)$ with the shortest Au(I)–Au(I) distance show emission and excitation at the longest wavelength.

Conclusions

We have demonstrated intense blue-to-yellow photoluminescence of the 1-D chain Au(I) complexes depending on their counteranion parts. As a consequence, the difference of counteranions provide diversity in the Au(I)–Au(I) distances of $[Au\{C(OMe)NHMe\}_2]^+(X^-)$ crystals, resulting in distinctive color variations from blue to yellow in photoluminescence of the $[Au\{C(OMe)NHMe\}_2]^+(X^-)$ complexes in the crystalline state.

Acknowledgment. We gratefully thank Mr. S. Katao and Mr. Y. Okajima, of the NAIST technical staff, for their technical support on regarding the X-ray single-crystal structural analysis and the time-resolved photoluminescence study. A part of this work was supported by a Grant-in-Aid for Scientific Research on an Innovative Area "Coordination Programming" (no. 2107) from the Ministry of Education, Culture, Sports, Science and Technology, MEXT, Japan. M.S. also thanks the MEXT, Japan for supporting the International Training Program, ITP, in NAIST and Mr. S. H. Lim for assistance.

Supporting Information Available: ^{1}H NMR spectra, MALDI-TOF mass spectra and photoluminescence decay profiles of $[Au\{C(OMe)NHMe\}_2]^+(X^-)$ ($X^- = CF_3SO_3^-$, PF_6^-, $CF_3CO_2^-$, ClO_4^- and I^-) complexes, and molecular packing diagrams and space-filling views of $[Au\{C(OMe)NHMe\}_2]^+(X^-)$ ($X^- = CF_3SO_3^-$, PF_6^-, and $CF_3CO_2^-$) complexes. Crystallographic information files (CIF) of $[Au\{C(OMe)NHMe\}_2]^+(X^-)$ ($X^- = CF_3SO_3^-$, PF_6^-, $CF_3CO_2^-$, ClO_4^-, and I^-) complexes. This material is available free of charge via the Internet at http://pubs.acs.org.

(38) Rios, D.; Olmstead, M. M.; Balch, A. L. *Dalton Trans.* **2008**, 4157–4164.